

Effect of van der Waals forces on the location of the critical point of a model molten salt

J. L. ArauzLara and M. MedinaNoyola

Citation: *The Journal of Chemical Physics* **82**, 4656 (1985); doi: 10.1063/1.448722

View online: <http://dx.doi.org/10.1063/1.448722>

View Table of Contents: <http://scitation.aip.org/content/aip/journal/jcp/82/10?ver=pdfcov>

Published by the [AIP Publishing](#)

Articles you may be interested in

[Secondary critical points in the supercritical region of a van der Waals fluid](#)

J. Chem. Phys. **88**, 2857 (1988); 10.1063/1.453975

[Critical behavior of the spin van der Waals model](#)

J. Math. Phys. **24**, 1927 (1983); 10.1063/1.525925

[Van der Waals Forces in Solids](#)

J. Chem. Phys. **43**, 1569 (1965); 10.1063/1.1696973

[Van der Waals Energy Changes in the Mixing of Molten Salts](#)

J. Chem. Phys. **36**, 1092 (1962); 10.1063/1.1732654

[On the Effects of Intramolecular van der Waals Forces](#)

J. Chem. Phys. **32**, 827 (1960); 10.1063/1.1730804



Effect of van der Waals forces on the location of the critical point of a model molten salt^{a)}

J. L. Arauz-Lara and M. Medina-Noyola

Centro de Investigación y de Estudios Avanzados del I. P. N., Departamento de Física, Apdo. Postal 14-740, 07000, México D. F.

(Received 20 November 1984; accepted 25 January 1985)

A mixture of charged hard spheres (restricted primitive model) with an attractive Yukawa tail added to represent van der Waals forces between the ions is considered as a model of molten salts. The location of the critical point of the gas-liquid phase transition is followed as a function of the strength A of the attractive term. It is found that the critical density increases with increasing A , but that a quantitative agreement between the theoretical results and the available experimental estimates of the critical constants for alkali halides requires the use of an effective dielectric constant greater than unity.

I. INTRODUCTION

It has been known¹ since 1970 that the restricted primitive model (RPM) of ionic solutions (neutral mixture of hard spheres of equal size and symmetric charge in a continuum of uniform dielectric constant) presents a phase transition between two fluid phases, with a critical point located in the low density-low temperature regime. After the findings of Vorontsov-Vel'yaminov *et al.*,¹ the location of the coexistence region was reported by Stell *et al.*² using several different approximations, which established this phenomenon as being a genuine property of the model rather than an artifact of the approximations involved in its description. Additional information has been provided in further research³⁻⁶ which complement the work of Stell *et al.* in deriving the coexistence curve from relatively simple analytic expressions of the equation of state. At the same time, the asymptotic properties of the structure of the model, as the critical point is approached, were studied by Medina-Noyola and McQuarrie⁵ in a simple extension of the Ornstein-Zernike theory of critical fluctuations. The main general consequence of this work, namely, the approximate equality between the like-and unlike-ions correlation functions at long distances near the critical point, have found additional support in the results of recent work of Medina-Noyola,⁷ who applied an extended version of the mean spherical approximation to the calculation of the thermodynamic and structural properties of the model in the low density-low temperature regime. These results also offer an indication that the process of ionic association constitute an essential feature of the structural properties of the model near the phase transition.

The phenomenon of ionic association and its relationship with the fluid phase transition of the restricted primitive model had been addressed before by Friedman and Larsen,⁸ who also discuss another important aspect, namely, the actual realization of this phase transition in real systems. They suggest that a number of experimental results involving ionic solutions and molten salts seem to satisfy a principle of corresponding states, for which the restricted primitive model provides a simple representation. Thus, they suggest that the fluid phase transition of the primitive model corresponds to

the gas-liquid phase transition of a molten salt, as well as to a phase transition involving a low-concentration, highly associated phase of an ionic solution and a more concentrated, almost fully ionized phase. According to Friedman and Larsen,⁸ the latter phase transition has been observed as a miscibility gap in certain electrolyte solution. It seems, however, that further theoretical and experimental work is needed to complement these suggestions with more precise quantitative comparisons.

The idea that the restricted primitive model is a rudimentary, but qualitatively precise representation of a real molten salt, and that the experimentally observed gas-liquid transition should have an image in the properties of the RPM was stated by Stillinger and Lovett,⁹ and was implicit in still previous theoretical work¹⁰ on molten salts. However, some reservations were expressed in this regard by Stell *et al.*² on the basis that the critical density of the fluid phase transition of the RPM, estimated in their work, is more than an order of magnitude lower than the critical density of the gas-liquid phase transition of a real molten salt. One could argue that the origin of this discrepancy is to be found in the difference between the RPM and the Hamiltonian of a real molten salt. This argument, however, would have to be complemented with the theoretical calculations of the location of the critical point for more realistic models, and its comparison with the corresponding experimental estimates.

A number of more realistic model potentials for a molten salt have been introduced in the literature,^{11,12} and much work has been done in the calculation of their properties by simulation and integral equation methods.^{11,12} Unfortunately, the use of these methods to locate the gas-liquid phase transition of such models would be rather expensive. However, a number of simplifications and approximations can be introduced to reduce the calculations to a reasonable level. In the models usually considered, three contributions to the interionic forces are included, namely, the impossibility of overlap of closed electron shells, the Coulombic interaction between the ionic charges, and the van der Waals dispersion forces. Among these three contributions, the first two are possibly the most essential, and they are already represented in the restricted primitive model by the hard-sphere and the Coulombic terms, respectively. van der Waals forces are

^{a)} Supported in part by COSNET/SEP and CONACyT.

generally described¹¹ by terms in the interionic potential with the form

$$u_{ij}^{\text{vdw}}(r) = -\frac{C_{ij}}{r^6} - \frac{D_{ij}}{r^8}.$$

Unfortunately, the addition of this terms to the Hamiltonian of the RPM would lead to a model with no particular analytic advantages. However, a fairly good fit of this function can be achieved by a somewhat simpler functional form, namely, a Yukawa function with amplitude and decay length determined in terms of C_{ij} and D_{ij} by some form of fitting procedure. If only a semiquantitative assessment of the effects of the van der Waals forces on the properties of the model is sought, this is indeed a good simplifying device, since, for example, the use of techniques such as the mean spherical approximation¹³ would reduce the numerical problem involved in the calculation of the structural and thermodynamic properties of the resulting model to a much more manageable level. Furthermore, with the same spirit, one could also neglect the difference between C_{11} , C_{12} , and C_{22} and between D_{11} , D_{12} , and D_{22} , so that the cation–cation, anion–anion, and cation–anion van der Waals forces are assumed to be identical, i.e., $C_{ij} = C$ and $D_{ij} = D$ for all i and j . This is, of course, a more drastic assumption (see Table I below) but given the rather gross inaccuracies in the available estimates¹¹ of the constants C_{ij} and D_{ij} , it is a fair simplifying assumption. In this work we shall use this simplification, and our estimate of the value of C will be taken as the direct average of the reported values of C_{11} , C_{12} , and C_{22} and similarly for D .

In this work we will use the simplifications just mentioned, and will consider the model resulting from adding an attractive Yukawa tail to the pair potential of the restricted primitive model. Such Yukawa term represents van der Waals interactions. Our aim is to calculate the change in the location of the critical point of the gas–liquid phase transition of the restricted primitive model when it is modified by the addition of a Yukawa tail representing van der Waals forces. This will give us some indication for the reason of the disagreement between the value of the critical constants predicted by the RPM and the corresponding experimental estimates for alkali halides. Our calculations are based on the model potential in Eq. (1) below, whose thermodynamic properties will be calculated with the use of the mean spherical approximation via the energy equation.¹³ In this manner we will determine the spinodal curve and the critical region for the model, and see how it is displaced when the attractive Yukawa tail is turned on. In the following section we outline the procedure of the calculation, and in Sec. III we present the results. Section IV is devoted to a semiquantitative comparison with available experimental data, and in Sec. V we summarize the conclusions.

II. RESTRICTED PRIMITIVE MODEL PLUS ATTRACTIVE YUKAWA TAIL

The model system that we wish to consider is defined by the following pairwise interionic potential:

$$u_{ij}(x) = u^{\text{HS}}(x) - A \frac{e^{-\alpha(x-1)}}{x} + \frac{e^2}{\epsilon\sigma} \frac{z_i z_j}{x} \quad (i, j = 1, 2), \quad (1)$$

where $x = r/\sigma$, σ being the hard sphere diameter, so that $u^{\text{HS}}(x) = 0$ for $x > 1$ and $= \infty$ for $x < 1$. The second term is meant to represent the van der Waals dispersion forces, A being a measure of its strength at contact, and α its inverse decay length which for simplicity are taken independent of i and j . z_i is the valence of the ions of species i ($z_1 = -z_2 = 1$) and e is the electronic charge. Because of electroneutrality, the number densities n_1 and n_2 of both ionic species are equal. ϵ is the dielectric constant of the uniform background. The interionic correlation functions $h_{ij}(x)$ will be obtained from the Ornstein Zernike equation, which reads¹³

$$h_{ij}(x) = c_{ij}(x) + \sum_{k=1}^2 n_k \int h_{ik}(|\mathbf{x} - \mathbf{x}'|) c_{kj}(x') d\mathbf{x}', \quad (2)$$

and will be complemented here by the mean spherical closure relation, namely,

$$c_{ij}(x) = +\beta A \frac{e^{-\alpha(x-1)}}{x} - \beta \frac{e^2}{\epsilon} \frac{z_i z_j}{x}, \quad x > 1. \quad (3a)$$

$$h_{ij}(x) = -1, \quad x < 1. \quad (3b)$$

From the solution of these equations, one obtains the radial distribution functions, $g_{ij}(x) = h_{ij}(x) + 1$, from which the thermodynamics follow via three, generally inconsistent routes,¹³ namely, the energy, virial, and compressibility equations. Of these three, the energy equation is well known to yield the most accurate approximation to the thermodynamic properties,²² and it will be used here. The energy equation reads

$$\frac{E}{N} = \frac{3}{2} k_B T + 12\eta \sum_{i,j} x_i x_j \int_0^\infty u_{ij}(x) g_{ij}(x) x^2 dx, \quad (4)$$

where $\eta = \pi n \sigma^3/6$, with $n = n_1 + n_2$, $x_i = n_i/n$, $N = nV$, and V being the volume of the system. E and T are the internal energy and temperature, and k_B is Boltzmann's constant.

In general, the correlation function $h_{ij}(x)$ is a symmetric matrix, and hence $h_{12}(x) = h_{21}(x)$. In addition, due to the symmetric roles that the positive and negative ions play in the interionic potential, we also have that $h_{11}(x) = h_{22}(x)$. Hence, we have to determine only two independent correlation functions, namely, $h_{11}(x)$ and $h_{12}(x)$. It is now convenient to introduce the sum and the difference between these two functions, which are proportional to the total number density and to the charge density correlation functions, respectively,

$$h^s(x) \equiv [h_{11}(x) + h_{12}(x)]/2, \quad (5a)$$

$$h^d(x) \equiv [h_{11}(x) - h_{12}(x)]/2. \quad (5b)$$

In terms of these two functions, we have that $h_{ij}(x)$ are given by

$$h_{ij}(x) = h^s(x) + z_i z_j h^d(x). \quad (6)$$

It is easy to show that the internal energy per particle is given, in terms of $h^s(x)$ and $h^d(x)$, using the explicit form of the pair potential in Eq. (1) by

$$\begin{aligned} \frac{E}{N} = & \frac{3}{2} k_B T - A e^\alpha 12\eta \int_0^\infty e^{-\alpha x} g^s(x) x dx \\ & + \left(\frac{e^2}{\epsilon\sigma} \right) 12\eta \int_0^\infty g^d(x) x dx, \end{aligned} \quad (7)$$

where $g^s(x) \equiv 1 + h^s(x)$ and $g^d(x) \equiv h^d(x)$. Thus, the contribution of the Yukawa and Coulombic interactions to the internal energy, are weighted, respectively, by $g^s(x)$ and $g^d(x)$. Similarly, we can show, using Eq. (6), that the Ornstein-Zernike equation [Eq. (2)] is equivalent to the following two integral equations:

$$h^s(x) = c^s(x) + (n\sigma^3) \int h^s(|\mathbf{x} - \mathbf{x}'|) c^s(x') d\mathbf{x}', \quad (8a)$$

$$h^d(x) = c^d(x) + (n\sigma^3) \int h^d(|\mathbf{x} - \mathbf{x}'|) c^d(x') d\mathbf{x}', \quad (8b)$$

where the particle-density and charge-density direct correlation functions are defined by

$$c^s(x) = [c_{11}(x) + c_{12}(x)]/2, \quad (9a)$$

$$c^d(x) = [c_{11}(x) - c_{12}(x)]/2. \quad (9b)$$

Using these definitions, we can see that the mean spherical closure relation [Eq. (3)] in this symmetric case can also be written as a closure relation for the Ornstein-Zernike equation for $h^s(x)$ in Eq. (8a), given by

$$c^s(x) = +\beta A \frac{e^{-\alpha(x-1)}}{x}, \quad x > 1, \quad (10a)$$

$$h^s(x) = -1, \quad x < 1 \quad (10b)$$

plus a closure relation for the Ornstein-Zernike equation for $h^d(x)$ in Eq. (8b) given by

$$c^d(x) = -\left(\frac{\beta e^2}{\epsilon\sigma}\right) \frac{1}{x}, \quad x > 1, \quad (11a)$$

$$h^d(x) = 0, \quad x < 1. \quad (11b)$$

We now notice that the integral Eq. (8a) with the closure relation in Eq. (10) is identical to the Ornstein-Zernike integral equation with the mean spherical closure for a one-component fluid of hard spheres with a Yukawa tail at number density n . The solution of such integral equation has been expressed in a variety of forms,¹⁴⁻¹⁶ and here we shall employ the results of the work of Høye and Blum.¹⁵ According to this work, the quantity γ , defined by

$$\gamma \equiv \frac{12\eta}{\alpha} \int_0^\infty dx x g^s(x) e^{-\alpha x}, \quad (12)$$

satisfies a quartic equation, with coefficients depending on η , α , and $A/k_B T$. In our calculations, two of the roots of such quartic equation were found to be complex for the range of interest of the parameters η , α , and A , and the physical branch was chosen so that in the limit $A \rightarrow 0$ the solution for the Percus-Yevick equation for hard spheres was obtained. As a check for our program, we used this solution for γ to evaluate the thermodynamic properties of the hard sphere plus Yukawa fluid and found agreement with the calculations of Henderson *et al.*¹⁶ In this manner, we obtained the second term of the right-hand side of Eq. (7) in terms of η , α , and A .

On the other hand, the solution of the integral equation for $h^d(x)$, Eq. (8b), with the closure relation in Eq. (11), is given by $h^d(x) = [h_{11}^{\text{pm}}(x) - h_{12}^{\text{pm}}(x)]/2$, where $h_{ij}^{\text{pm}}(x)$ are the interionic correlation functions of the restricted primitive model within the mean spherical approximation, whose solution was given by Waisman and Lebowitz,¹⁷ who also

find an explicit expression for the integral that appears in the right-hand side of Eq. (7), namely,

$$\int_0^\infty g^d(x) x dx = -(y + 1 - \sqrt{1 + 2y})/12\eta y, \quad (13)$$

where

$$y^2 \equiv \sigma^2 \kappa_D^2 = \sigma^2 \left(\frac{4\pi\beta n e^2}{\epsilon} \right). \quad (14)$$

Thus, the excess internal energy per particle for our system, defined as $E^{\text{ex}}/N = E/N - \frac{3}{2} k_B T$, is given by the last two terms of Eq. (7) which can be written as

$$\begin{aligned} \frac{E^{\text{ex}}}{N} = & -\alpha e^2 A \gamma \left(\eta, \frac{A}{k_B T}, \alpha \right) \\ & - \left(\frac{e^2}{\epsilon\sigma} \right) (y + 1 - \sqrt{1 + 2y})/y \end{aligned} \quad (15)$$

with γ being the physical solution of the quartic equation derived by Høye and Blum¹⁵ and y being defined in Eq. (14). From the excess internal energy we can derive other thermodynamic properties. In particular, we are interested here in the equation of state, i.e., $p = p(n, T)$. This is given by

$$p(n, T) = p^{\text{HS}}(n, T) + n^2 k_B T \int_0^\beta \left[\frac{\partial}{\partial n} (E^{\text{ex}}(n, \beta')/N) \right] d\beta', \quad (16)$$

where $p^{\text{HS}}(n, T)$ is the pressure of the reference hard-sphere system and $\beta = 1/k_B T$. Since we are interested in determining the location of the critical point and the spinodal curve, i.e., the points at which $(\partial p/\partial n)_T = 0$, we need to evaluate

$$\left(\frac{\partial p}{\partial n} \right)_T = \left(\frac{\partial p}{\partial n} \right)_T^{\text{HS}} + k_B T \int_0^\beta \left[\frac{\partial}{\partial n} n^2 \frac{\partial}{\partial n} \left(\frac{E^{\text{ex}}}{N} \right) \right] d\beta'. \quad (17)$$

The use of Eq. (15) allows us to rewrite this equation as

$$\begin{aligned} \beta \left(\frac{\partial p}{\partial n} \right)_T = & \beta \left(\frac{\partial p}{\partial n} \right)_T^{\text{HS}} \\ & + \frac{y}{48\eta} [1 - \sqrt{1 + 2y} + y/\sqrt{1 + 2y}] \\ & - \alpha e^2 A \int_0^\beta \left[\frac{\partial}{\partial \eta} \eta^2 \frac{\partial}{\partial \eta} \gamma(\eta, \beta', A, \alpha) \right] d\beta'. \end{aligned} \quad (18)$$

For $\beta(\partial p/\partial n)^{\text{HS}}$ we use Carnahan-Starling's equation of state for the hard sphere fluid,

$$\beta \left(\frac{\partial p}{\partial n} \right)^{\text{HS}} = \frac{1 + 4\eta + 4\eta^2 - 4\eta^3 + \eta^4}{(1 - \eta)^4}. \quad (19)$$

In the absence of electrostatic and Yukawa interactions, $\beta(\partial p/\partial n)_T = \beta(\partial p/\partial n)_T^{\text{HS}}$ is always positive, and no fluid phase transition is possible. With the electrostatic term also included, Eq. (18) has been used⁵ to estimate the location of the critical point of the restricted primitive model, with the following results: $\epsilon k_B T_c \sigma / e^2 = 78.5 \times 10^{-3}$ and $\eta_c = 0.73 \times 10^{-2}$. Similarly, for the fluid of hard-spheres plus Yukawa tail, the use of Eq. (18) without the electrostatic term leads to the determination of the spinodal curve and the critical point. For example, with $\alpha = 1.8$, we get $k_B T_c /$

$A = 1.24$ and $\eta_c = 0.17$, which are in agreement with the calculations of Henderson *et al.*¹⁶ In our use of Eq. (18) we have expressed first the integrand of the third term as a function of γ itself and of the coefficients of the quartic equation that γ satisfies, which are functions of η , β , A , and α . Thus, we avoid a numerical algorithm for the two derivatives involved. However, the integration of β was carried out numerically.

III. SPINODAL CURVE AND CRITICAL POINT OF THE RPM PLUS YUKAWA TAIL

We now show the results of our calculations of the spinodal curve of the restricted primitive model plus attractive Yukawa tail defined in Eq. (1). The parameters A and α are determined by fitting the van der Waals potential,

$$u_{ij}^{\text{vdw}}(r) = -\frac{C}{r^6} - \frac{D}{r^8}, \quad (20)$$

with the Yukawa term of Eq. (1), by imposing the following conditions:

$$u_{ij}^{\text{vdw}}(\sigma) = -\frac{C}{\sigma^6} - \frac{D}{\sigma^8} = -A \quad (21)$$

and

$$\int_1^\infty \left(\frac{C/\sigma^6}{x^6} + \frac{D/\sigma^8}{x^8} \right) x^2 dx = \int_1^\infty \left(\frac{A e^{-\alpha(x-1)}}{x} \right) x^2 dx. \quad (22)$$

Equation (21) requires the fitting Yukawa curve to coincide with the van der Waals potential at $r = \sigma$, whereas Eq. (22) requires that the volume integral of the van der Waals potential in the region $r > \sigma$ be the same as the corresponding integral of the fitting Yukawa function. Thus, A and α are given in terms of C , D , and σ by

$$A = (C/\sigma^6) + (D/\sigma^8) \quad (23)$$

and

$$\alpha = \alpha_1 + (\alpha_1^2 + 2\alpha_1)^{1/2} \quad (24)$$

with

$$\alpha_1 \equiv \frac{2}{3} (C + D/\sigma^2)/(C + 3D/5\sigma^2). \quad (25)$$

This we found to be a very effective systematic way of carrying out the fitting for all the values of the parameters C , D , and σ of interest.

The values used here for the constants C , D , and σ were based on the results available in the literature for C_{ij} , D_{ij} and σ_i for KCl. Unfortunately, there are rather gross discrepancies between such results, as illustrated in Table I, where the estimates of Mayer^{11,18} and of Jain *et al.*¹⁹ for C_{ij} and D_{ij} for KCl are summarized (here species 1 corresponds to the cations). As can be seen from these results, the values of the constants C_{ij} and D_{ij} are not independent of i and j for KCl, but still define our constants C and D as the direct average $(C_{11} + C_{12} + C_{22})/3$ and $(D_{11} + D_{12} + D_{22})/3$, respectively. These are also listed in Table I, from which we notice that we should consider values of C at least in the range $C_M < C < C_J$ and of D in the range $D_M < D < D_J$, where C_M and D_M correspond to Mayer's results, and C_J and D_J to the results of Jain *et al.* Similarly, the value of $\sigma = (\sigma_1 + \sigma_2)/2$ is not exactly

TABLE I. Estimates of the van der Waals constants C_{ij} and D_{ij} reported by Mayer [Ref. (18)] and by Jain *et al.* [Ref. (19)]. C_{ij} is given in units of 10^{-60} erg cm⁶ and D_{ij} in 10^{-76} erg cm.⁸ The columns labeled C and D correspond to the average C_{ij} and D_{ij} in the same line.

	C_{11}	C_{12}	C_{22}	D_{11}	D_{12}	D_{22}	C	D
Mayer Ref. 18	24.3	48	124.0	24	73	250	65.4	115.6
Jain <i>et al.</i> Ref. 19	71	125	242	60	139	330	146	176.3

determined, and we shall consider values of σ for KCl between $\sigma_m = 2.5 \text{ \AA}^{20}$ and $\sigma_M = 3.05 \text{ \AA}^{11}$. Thus, the values of α and A are subject to uncertainties, and in Fig. 1 we illustrate the region of the (α, A) plane consistent with the ranges of variation for C , D , and σ mentioned above. In Fig. 1 we have introduced the parameter R defined as

$$R = A/(e^2/\epsilon\sigma), \quad (26)$$

which is the strength of the Yukawa potential at contact A in units of the strength of the Coulombic potential at contact $(e^2/\epsilon\sigma)$. From Fig. 1, we can see that a reasonable estimate for α is $\alpha \approx 4$, whereas values of R between 0.01 and 0.08 should be considered. We have calculated the spinodal curve by locating the values of the inverse reduced temperature $\beta^* \equiv e^2/\epsilon k_B T \sigma$ and of the reduced density $\eta \equiv \pi n \sigma^3/6$ at which the derivative $(\partial p/\partial n)_T$ calculated according to Eq. (18), equals zero. Different spinodal curves will be obtained for different values of α and R . Thus, for $R = 0$ we have the results for the RPM. In Fig. 2 we show this spinodal curve, in the plane (η, β^*) as the curve labeled $R = 0$. In that figure we also show the spinodal curve for $\alpha = 4$ and $R = 0.08$. The broken line indicates the displacement of the critical point when the value of R is increased from zero (critical point of the RPM) to $R = 0.12$ keeping fixed the value of $\alpha = 4$.

As can be noticed from Fig. 2, η_c is found to increase as the van der Waals interaction increases. In fact, the value of η_c changes by an order of magnitude when R increases from

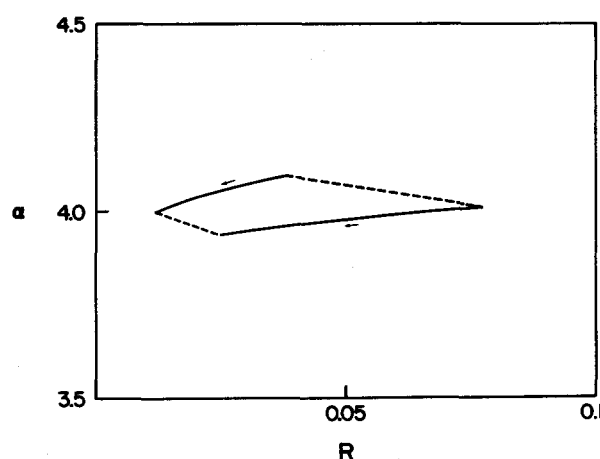


FIG. 1. Region of the plane (R, α) corresponding to the points obtained from Eqs. (23)–(25) for $2.5 \text{ \AA} < \sigma < 3.05 \text{ \AA}$, $C_M < C < C_J$ and $D_M < D < D_J$. The upper solid curve corresponds to $C = C_M$ and $D = D_M$ with the arrow indicating the direction of increasing values of σ . The lower solid curve correspond to $C = C_J$ and $D = D_J$. The broken lines are only meant to define a closed region, and do not correspond to fixed values of σ .

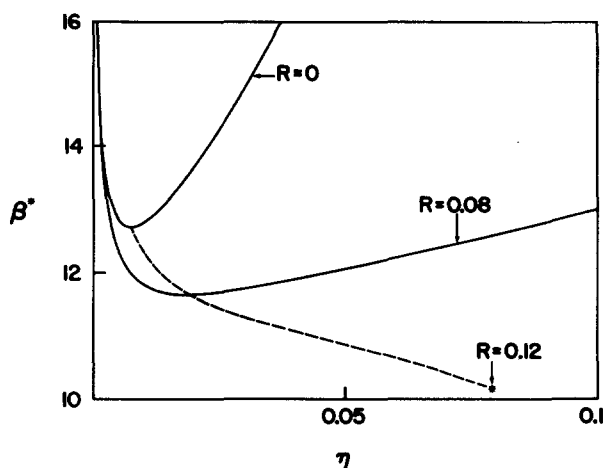


FIG. 2. Spinodal curves for the restricted primitive model with Yukawa tail corresponding to $\alpha = 4$ and the values $R = 0$ (restricted primitive model) and $R = 0.08$. The broken curve gives the location of the critical point when R is varied in the interval $0 < R < 0.12$.

zero to 0.12. On the other hand, β_c^* is observed to decrease with increasing R , a result that is expected since a higher kinetic energy is required to overcome the additional average attraction between the ions due to the van der Waals interactions. The increase in η_c with R indicates that the absence of van der Waals force in the restricted primitive model is one of the reasons for the very small values of η_c , and the results in this section illustrate the fact that van der Waals forces produce a net effect of increasing the critical density. However, the actual comparison with the available experimental information suggests that still other effects are being left out by the model. This is discussed in the following section.

IV. COMPARISON WITH EXPERIMENTAL ESTIMATES

The direct experimental determination of the critical point of molten alkali halides is prevented by the high values of the critical temperature. However, indirect estimates based on the law of rectilinear diameters²¹ predict, for KCl, a critical temperature of about $T_c^{\text{expt}} \approx 3200$ K and a critical density $D_c^{\text{expt}} \approx 0.18$ g/cm³, corresponding to a critical number density $\eta_c = 2.9 \times 10^{21}$ /cm³. Although the uncertainties of these estimates are not well established, we shall adopt them as the best available experimental values. These results can be used to calculate the experimental estimate of $\beta_c^* = e^2/\epsilon k_B T_c^{\text{expt}} \sigma$ and $\eta_c \equiv \pi n_c^{\text{expt}} \sigma^3/6$. Taking $\epsilon = 1$, and varying σ in the range $2.5 \text{ \AA} \leq \sigma \leq 3.05 \text{ \AA}$, we obtain the curve AB in Fig. 3. In the same figure, we also indicate the location of the critical point of the RPM (point P in the figure). We observe that the reduced critical constants η_c and β_c^* of the RPM lie totally displaced from the range consistent with the experimental estimates. We now ask to what extent including van der Waals forces may lead to closer agreement between the theoretical predictions and the experimental estimates. As we saw in the last section, the calculated η_c increases with R , and the largest values of R are obtained with the use of C_J and D_J with $\sigma = 2.5 \text{ \AA}$. In Fig. 3, the curve CD represents the position of the critical point of the RPM plus Yukawa tail with $C = C_J$ and $D = D_J$, and with σ varying in

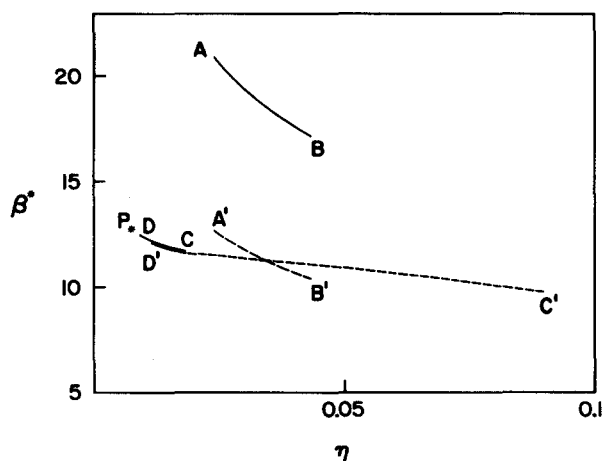


FIG. 3. Position of the critical point in the plane (η, β^*) . The curve AB represents the experimental values of $\beta_c^* = q^2/\epsilon k_B T_c \sigma$ and $\eta = \pi n_c/6$ with $T_c = 3200$ K, $n_c = 2.9 \times 10^{21}$ /cm³ (values reported in Ref. 21), $\epsilon = 1$, and varying σ in the interval $\sigma_A = 2.5 \text{ \AA} < \sigma < 3.05 \text{ \AA} \equiv \sigma_B$. Curve A'B' was obtained similarly, but with $\epsilon = 1.65$. The theoretical values with $\epsilon = 1$ fall in the curve CD (with $\sigma_c = 2.5 \text{ \AA}$), and with $\epsilon = 1.65$, in the curve C'D'. The point labeled P corresponds to the critical point of the restricted primitive model, without van der Waals forces.

the range $2.5 \text{ \AA} \leq \sigma \leq 3.05 \text{ \AA}$. Again, we notice that even not yet an overlap between the theoretical and experimental ranges of η_c corresponding to the region of small values of σ , and the disagreement in β_c^* continues to be substantial. However, it is interesting to notice that almost complete agreement can be achieved if values of the dielectric constant ϵ different than 1 are considered. To illustrate this, we show in Fig. 3 the curve A'B' obtained in a similar way as AB but using a dielectric constant $\epsilon = 1.65$. In this case, this is equivalent to a simple reduction of β_c^* by a factor $1/\epsilon$. On the other hand, considering $\epsilon \neq 1$ has dramatic consequences in the value of the critical constants η_c and β_c^* calculated from our model. This is due to the fact that even though α and A do not depend on ϵ , the ratio $R \equiv A/(e^2/\epsilon \sigma)$ does, and this is a parameter on which η_c and β_c^* depend sensitively. In Fig. 3 we also illustrate the results corresponding to curve CD, but calculated with $\epsilon = 1.65$. This curve is labeled C'D'. We now find that, within the uncertainties considered for σ , the theoretical and experimental estimates of the location of the critical point are in much better agreement. We find that the crossing of A'B' and C'D' corresponds to $\sigma = 2.66 \text{ \AA}$ with the other parameters being $C = C_J$, $D = D_J$, and $\epsilon = 1.65$. This, however, is not a unique way to compare the experimental values with our theoretical results, and other sets of values for these parameters may lead to similar consistency. However, our purpose here is only to indicate that if quantitative comparisons between experimental results and theoretical calculations based in the model considered here will probably require in general the use of an effective dielectric constant as a fitting parameter.

V. CONCLUSIONS

In this paper we have indicated a simple approach to the thermodynamic properties of the restricted primitive model plus a Yukawa tail, based on the mean spherical approxima-

tion and the energy equation. We have employed this approach to calculate the critical point and the spinodal curve of the gas-liquid phase transition of the model. Our main goal was to see how the position of the critical point changes as the amplitude of the Yukawa tail was varied, so as to have an indication of the importance of van der Waals forces in determining the values of the critical constants. We found that the most noticeable consequence was an increase of the reduced critical density with increasing strength of the van der Waals interactions. This observation may serve as an indication that the neglect of such attractive force is the origin for the rather gross discrepancies between the experimental estimates of the critical density and the theoretical predictions, based on the restricted primitive model. However, we also find that the discrepancies in the value of the reduced temperatures are still substantial, indicating that still other important features of the Hamiltonian of real molten salt are being neglected. Here we have considered the possibility of establishing a practical comparison between theoretical and experimental results, based on the idea of using ϵ , the dielectric constant, as a fitting parameter. This could be rationalized as an effect of the nonzero polarizability of the electronic cloud of each ion. However, a simple estimate of the effective dielectric constant based on the Clausius-Mosotti equation, cannot justify $\epsilon \approx 1.65$ which is the value of our fitted effective dielectric constant. Thus, other effects, such as ionic association,^{4,6} would have to be considered, if we wished to give a less empirical character to our comparison at the end of Sec. IV. However, given the large uncertainties in the experimental estimates and the acknowledged primitivity of our model, we believe that further

refinements of this type of comparison will have to be based on more sophisticated models, approximations, and numerical procedures.

- ¹P. N. Vorontsov-Vel'yaminov, A. M. El'yashevich, L. A. Morgenshtern, and V. P. Chassovskikh, *Teplofiz. Vys. Temp.* **8**, 277 (1970).
- ²G. Stell, K. C. Wu, and B. Larsen, *Phys. Rev. Lett.* **37**, 1369 (1976).
- ³M. Robere, R. Miniero, M. Parrinello, and M. P. Tosi, *Phys. Chem. Liq.* **9**, 11 (1979).
- ⁴W. Ebeling and M. Grigo, *Ann. Physik* **37**, 21 (1980).
- ⁵M. Medina-Noyola and D. A. McQuarrie, *J. Stat. Phys.* **18**, 445 (1978).
- ⁶M. J. Gillan, (a) *Mol. Phys.* **41**, 75 (1980); (b) *Mol. Phys.* **49**, 421 (1983).
- ⁷M. Medina-Noyola, *J. Chem. Phys.* **81**, 5059 (1984).
- ⁸H. L. Friedman and B. Larsen, *J. Chem. Phys.* **70**, 92 (1979).
- ⁹F. Stillinger and R. Lovett, *J. Chem. Phys.* **48**, 3858 (1968).
- ¹⁰(a) D. A. McQuarrie, *J. Phys. Chem.* **66**, 1508 (1962); (b) C. M. Carlson, H. Eyring, and T. Ree, *Proc. Nat. Acad. Sci.* **46**, 333 (1960).
- ¹¹M. J. L. Sangster and M. Dixon, *Adv. Phys.* **25**, 247 (1976).
- ¹²L. V. Woodcock, *Advances in Molten Salt Chemistry*, edited by J. Braunstein *et al.* (Plenum, New York, 1975), Vol. 3.
- ¹³J. P. Hansen and I. R. McDonald, *Theory of Simple Liquids* (Academic, London, 1976).
- ¹⁴E. Waisman, *Mol. Phys.* **25**, 45 (1973).
- ¹⁵J. S. Høye and L. Blum, *J. Stat. Phys.* **16**, 399 (1977).
- ¹⁶D. Henderson, E. Waisman, J. L. Lebowitz, and L. Blum, *Mol. Phys.* **35**, 241 (1978).
- ¹⁷E. Waisman and J. L. Lebowitz, *J. Chem. Phys.* **56**, 3093 (1972).
- ¹⁸J. E. Mayer, *J. Chem. Phys.* **1**, 270 (1933).
- ¹⁹J. K. Jain, J. Shanker, and D. P. Khandelwal, *Phys. Rev. B* **13**, 2692 (1976).
- ²⁰M. C. Abramo, C. Caccamo, G. Pizzimenti, M. Parrinello, and M. P. Tosi, *J. Chem. Phys.* **68**, 2889 (1978).
- ²¹A. D. Kieschenbaum, J. A. Cahill, P. J. McGonigal, and A. V. Grosse, *J. Inorg. Nucl. Chem.* **24**, 1287 (1962).
- ²²See, however, Ref. 6(a) for a discussion on the accuracy of this approximation as applied to the restricted primitive model. Reference 6(b) discusses corrections to these results due to ionic association, which is not adequately described by the MSA.